

Surface density of states of s_{\pm} -wave Cooper pairs in a two-band model

Seiichiro Onari and Yukio Tanaka
Department of Applied Physics, and JST, TRIP,
Nagoya University, Chikusa, Nagoya 464-8603, Japan.

We calculate the surface density of state (SDOS) of s_{\pm} -wave Cooper pair in two-band superconductor model, where gap functions have different signs between two bands. We find that the Andreev bound state appears at surface due to the sign change in the gap function in the interband quasiparticle scattering. However, we do not obtain the zero-energy peak of SDOS in contrast to the d -wave case. The tunneling spectroscopy of s_{\pm} -wave is much more complex as compared to the d -wave case realized in high- T_c cuprates.

PACS numbers: 74.50.+r, 74.20.-z, 74.25.Jb

Keywords: Unconventional superconductivity, two-band model, Tunneling spectroscopy

I. INTRODUCTION

Recent discovery of superconductivity in the iron based LaFeAsO $_{1-x}$ F $_x$ with $T_c = 26\text{K}$ ¹ has aroused great interests as a class of non-cuprate compound. In the iron-based family, various compounds exhibit superconductivity with T_c now exceeding 55 K. Superconductivity has also been found in iron-based materials with different layered structures that include BaFe $_2$ As $_2$ ² and FeSe³. Local spin-density calculations for LaFeAsO have shown that the system is around the border between magnetic and nonmagnetic states, with a tendency toward antiferromagnetism.^{4,5} It has also been pointed out that the electron-phonon coupling in this material is too weak to account for $T_c = 26\text{K}$.^{6,7} Based on the first principles calculation, minimum five-band model to describe the iron-based superconductor has been proposed⁸. Using this five-band model, pairing symmetry has been calculated based on the random phase approximation (RPA)⁸. The resulting gap function does not have nodes on the Fermi surface while it has a sign change between Fermi surfaces. Now, it is called an s_{\pm} -wave pairing^{9,10}. There have also been relevant theoretical predictions which support the realization of the s_{\pm} -wave model^{11,12,13}.

In order to elucidate the energy-gap structure of these s_{\pm} -wave superconductors, experiments based on standard technique, *e.g.*, NMR^{14,15}, specific heat⁶, penetration depth^{16,17} and quasiparticle tunneling spectroscopy have started^{18,19,20,21}. It is a very challenging issue to clarify the superconducting profile of s_{\pm} -wave superconductors. Since the internal phase degree of freedom exists in the gap function of s_{\pm} -wave pairing, it is natural to expect phase sensitive phenomena realized in high- T_c cuprates^{22,23,24,25}. As shown in the study of high- T_c cuprates, the mid gap Andreev bound state (MABS) is formed at the surface due to the internal phase effect, where a quasiparticle feels a different sign of the gap function depending on the direction of their motions. The presence of the MABS produces zero-energy peak (ZEP) of the surface density of states (SDOS) and has been observed as a zero-bias conductance peak (ZBCP) in tunneling spectroscopy up to now^{26,27,28,29}. It is an un-

gent topic to reveal whether MABS exists in the s_{\pm} -wave pairing or not.

Several theories of surface or interface profiles about s_{\pm} -wave pairing have been presented very recently^{30,31,32,33,34,35,36,37}. However, SDOS of two-band superconductors with s_{\pm} model has not been understood yet. The presence or absence of MABS have not been resolved yet. Furthermore, character of the nonzero inner gap Andreev bound state (ABS) has not been clarified. To reply to these issues, in the present paper, we employ a simple two-band tight-binding model with s_{\pm} -wave as a prototype of iron-based pnictides, and calculate SDOS for the [100] and [110] oriented interfaces using the t-matrix method³⁸. A merit of our calculation is that details of the band structure and band mixing can be microscopically taken into account. We find that ABS with nonzero energy is formed at the surface due to the interband quasiparticle scattering, through which gap functions change sign. However, there is no ZEP in SDOS in contrast to the case of d -wave pairing realized in high- T_c cuprates^{26,27,28}.

II. MODEL AND FORMULATION

We start with a two-band tight-binding model on a square lattice. Since there has not been an explicit study about the SDOS of the s_{\pm} model, we choose the energy dispersion of two orbitals simply supposing d_{xz} and d_{yz} orbitals or p_x and p_y orbitals. Hereafter, we define index 1 in matrix form as d_{xz} (p_x) orbital and index 2 as d_{yz} (p_y) orbital. X and Y axes are rotated by 45 degrees from x - y , where x and y denote the axes in a unit cell as shown in Fig. 1.

First, we discuss the normal state. Tight-binding Hamiltonian is given in the form

$$H_0 = \sum_{ij} \sum_{\mu\nu} \sum_{\sigma} t_{i\mu,j\nu} c_{i\mu\sigma}^{\dagger} c_{j\nu\sigma}, \quad (1)$$

where $t_{i\mu,j\nu}$ is a hopping integral from the ν -th orbital on the j -th site to the μ -th orbital on the i -th site, $c_{i\mu\sigma}^{\dagger}$ creates an electron with spin σ on the μ -th orbital at

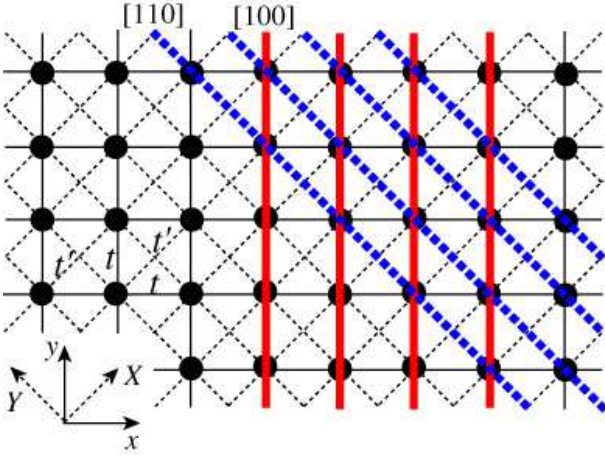


FIG. 1: (Color online) Two-dimensional square lattice with nearest-neighbor hopping t (thin solid line) and next-nearest-neighbor hopping t' (thin dotted line). The [100] and [110] oriented surfaces are constructed by inserting four infinite potential barriers illustrated with thick solid lines and thick dotted lines, respectively

site i . As shown in Fig. 1, we take the nearest-neighbor hopping t and the next-nearest-neighbor hopping t' . The band filling n is defined as the number of electrons per number of sites (e.g., $n = 1$ for half filling). The Hamiltonian in the Fourier transformed representation is given as

$$H_0 = \sum_{\mathbf{k}} \sum_{\mu\nu} \sum_{\sigma} \hat{\varepsilon}_{\mu\nu}^0(\mathbf{k}) c_{\mathbf{k}\mu\sigma}^\dagger c_{\mathbf{k}\nu\sigma}, \quad (2)$$

where the 2×2 matrix $\hat{\varepsilon}^0(\mathbf{k})$ is denoted by

$$\hat{\varepsilon}^0(\mathbf{k}) = \begin{pmatrix} -t \cos k_x & 2t' \sin k_x \sin k_y \\ 2t' \sin k_x \sin k_y & -t \cos k_y \end{pmatrix}. \quad (3)$$

Hereafter, we take t and the lattice constant a as the units for energy and length, respectively. $\hat{\varepsilon}^0(\mathbf{k})$ can be diagonalized to $\varepsilon_a^0(\mathbf{k})$, which corresponds to the energy of band a

$$\varepsilon_a^0(\mathbf{k}) = \sum_{\mu\nu} U_{\mu a}^*(\mathbf{k}) U_{\nu a}(\mathbf{k}) \hat{\varepsilon}_{\mu\nu}^0(\mathbf{k}), \quad (4)$$

where $U(\mathbf{k})$ is a 2×2 unitary matrix. Fermi surfaces consist of two parts near the half filling as shown in Fig. 2. We define the band which forms inner (outer) Fermi surface as band $- (+)$.

In a two-band model, gap function generally forms a 2×2 matrix. The gap function $\hat{\Delta}_{\mu\nu}(\mathbf{k})$ in the orbital representation is transformed to the gap function $\Delta_{ab}(\mathbf{k})$ in the band representation using the unitary matrix $U(\mathbf{k})$,

$$\Delta_{ab}(\mathbf{k}) = \sum_{\mu\nu} U_{\mu a}^*(\mathbf{k}) U_{\nu b}(-\mathbf{k}) \hat{\Delta}_{\mu\nu}(\mathbf{k}). \quad (5)$$

Here, we neglect the frequency ω dependence of the gap function and assume that the gap function in the band

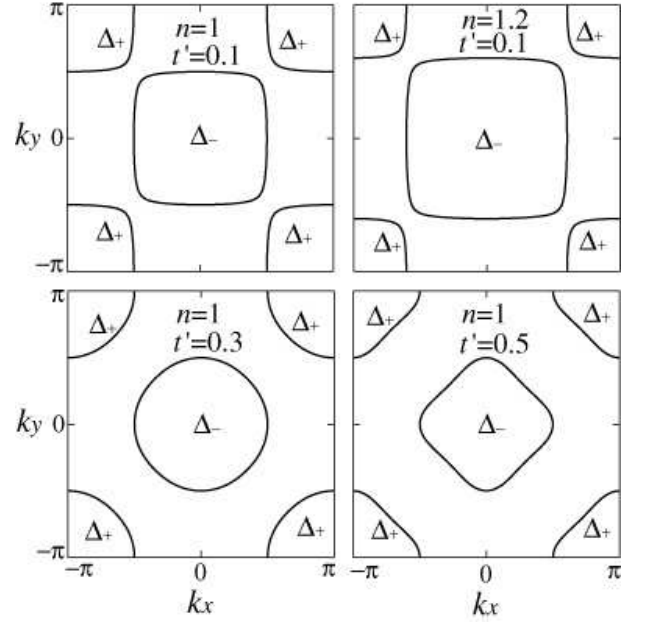


FIG. 2: Outer (inner) Fermi surfaces with gap function $\Delta_{+(-)}$ consist of band $+(-)$.

representation is diagonal, $\Delta_a(\mathbf{k}) = \Delta_{aa}(\mathbf{k})$. Gap function of band $-$ (inner Fermi surface) and band $+$ (outer Fermi surface) are denoted by Δ_- and Δ_+ , respectively as shown in Fig. 2. Then, the gap function in the orbital representation is obtained as

$$\hat{\Delta}_{\mu\nu}(\mathbf{k}) = \sum_a U_{\mu a}(\mathbf{k}) U_{\nu a}(-\mathbf{k}) \Delta_a(\mathbf{k}). \quad (6)$$

In the case that the hopping integral is given by a real number, the relation $\hat{\varepsilon}_{\mu\nu}^0(\mathbf{k}) = \hat{\varepsilon}_{\mu\nu}^{0*}(-\mathbf{k})$ is satisfied. Then, we take following relation

$$U_{\mu a}(\mathbf{k}) = U_{\mu a}^*(-\mathbf{k}). \quad (7)$$

Using the above gap function, bulk Green's function $\hat{G}(\omega, \mathbf{k})$ in the superconducting state is given by a 4×4 Nambu representation as follows

$$\hat{G}(\omega, \mathbf{k}) = \left[\omega - \begin{pmatrix} \hat{\varepsilon}^0(\mathbf{k}) - \mu & \hat{\Delta}(\mathbf{k}) \\ \hat{\Delta}^\dagger(\mathbf{k}) & -\hat{\varepsilon}^0(\mathbf{k}) + \mu \end{pmatrix} \right]^{-1}, \quad (8)$$

with chemical potential μ . In the actual numerical calculation, we replace ω by $\omega + i\gamma$ with small real number γ to avoid divergence of the integral. Local density of states (LDOS) in the bulk is obtained by $-1/(N\pi) \sum_{\mathbf{k}, l=1,2} \text{Im} \hat{G}_{ll}(\omega, \mathbf{k})$, where N denotes \mathbf{k} -point meshes. The Green's function of the inhomogeneous system including surface $\hat{G}^s(\omega, \mathbf{r}, \mathbf{r}')$ is calculated by $\hat{G}(\omega, \mathbf{r})$, which is the Fourier transformed form of $\hat{G}(\omega, \mathbf{k})$. As shown in Fig. 1, we insert the infinite potential barrier $Z(\mathbf{r})$ in four-atomic layers parallel to the

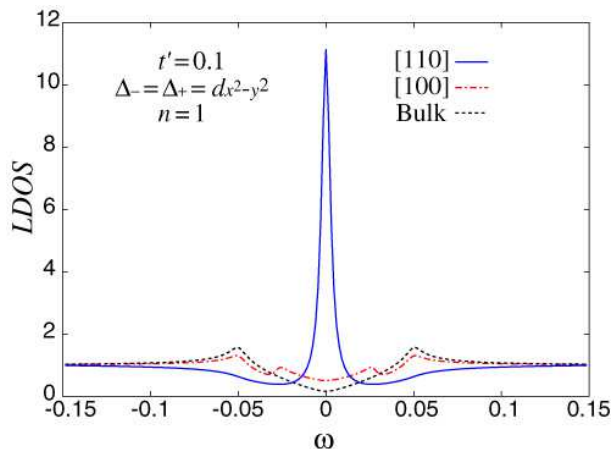


FIG. 3: (Color online) SDOS of the [110] and [100] oriented surfaces and LDOS in bulk are depicted with solid line, dashed-dotted line and dotted line, respectively for $n = 1$, $t' = 0.1$, and $\Delta_- = \Delta_+ = 0.05(\cos k_x - \cos k_y)$ ($d_{x^2-y^2}$ -wave). These values are normalized by the values in the normal state.

surface in the actual calculation. $\hat{G}^s(\omega, \mathbf{r}, \mathbf{r}')$ is given by

$$\hat{G}^s(\omega, \mathbf{r}, \mathbf{r}') = \hat{G}(\omega, \mathbf{r} - \mathbf{r}') + \int d\mathbf{r}'' \hat{G}(\omega, \mathbf{r} - \mathbf{r}'') Z(\mathbf{r}'') \hat{\tau}_3 \hat{G}^s(\omega, \mathbf{r}'', \mathbf{r}')$$

where $\hat{\tau}$ denotes the Pauli matrix in charge space. We note that \hat{G}^s breaks translational symmetry. Using the $\hat{G}^s(\omega, \mathbf{r}, \mathbf{r}')$, we obtain SDOS by $-1/\pi \sum_{l=1,2} \text{Im} \hat{G}_{ll}^s(\omega, \mathbf{r}_s, \mathbf{r}_s)$, where \mathbf{r}_s denotes the location of the surface. Throughout this study, we take $N = 4096 \times 4096$ \mathbf{k} -point meshes and $\gamma = 0.003$.

III. RESULT

In the following, we focus on LDOS at the surface, i.e., SDOS and bulk. First we show the result of the $d_{x^2-y^2}$ -wave case for $n = 1$, $t' = 0.1$ in Fig. 3, where the gap function of band $+(-)$ is chosen as $\Delta_{+(-)} = 0.05(\cos k_x - \cos k_y)$. Throughout the present study, LDOS is normalized to that of the value in the normal state at $\omega = 0$. We see a sharp ZEP of SDOS in [110] oriented surface and V-shaped LDOS in the bulk, which are consistent with the case of the single band $d_{x^2-y^2}$ -wave^{26,27,28}. The origin of the sharp ZEP is the sign change in the gap function felt by quasiparticles scattered at the surface, where the momentum of the quasiparticles parallel to the [110] surface is conserved^{26,27,28}.

As a reference, we show the result of s -wave pairing in Fig. 4, where $n = 1$, $t' = 0.1$ and $\Delta_- = \Delta_+ = 0.1$. The line shapes of SDOS of the [100] and [110] oriented surfaces, and LDOS of bulk are almost identical. This behavior is robust irrespectively of the band structure as far as the relation $\Delta_- = \Delta_+$ is satisfied.

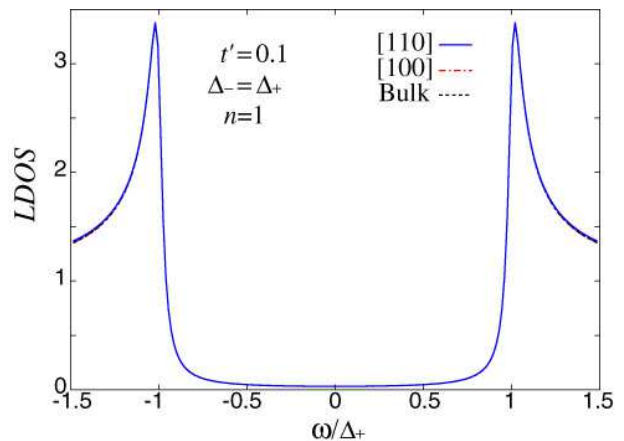


FIG. 4: (Color online) Plots of LDOS similar to Fig. 3 for $n = 1$, $t' = 0.1$, and $\Delta_- = \Delta_+ = 0.1$ (s -wave).

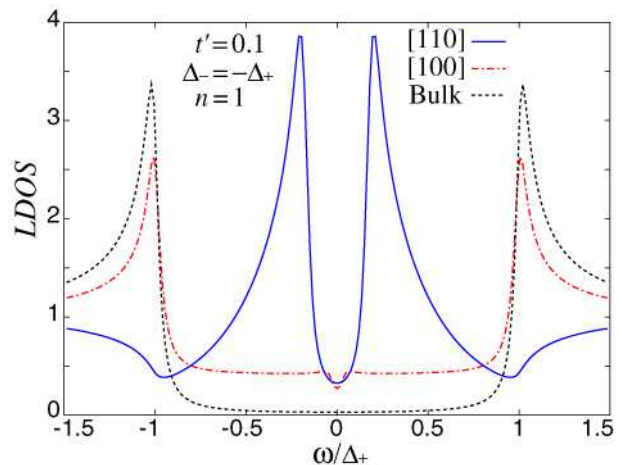


FIG. 5: (Color online) Plots of LDOS similar to Fig. 3 for $n = 1$, $t' = 0.1$, and $\Delta_- = -\Delta_+ = -0.1$ (s_{\pm} -wave).

Next, we move to the s_{\pm} -wave case. The corresponding results for s_{\pm} -wave with $n = 1$, $t' = 0.1$ are shown in Fig. 5, where we choose $\Delta_{+(-)} = +(-)0.1$. We see that two sharp peaks within the bulk energy gap appear in the [110] oriented SDOS³¹. The clear difference from Fig.3 is that there is no ZEP. For the [100] oriented surface, the value of the corresponding SDOS within the gap is almost constant with nonzero value.

In order to clarify the origin of the two peaks in SDOS of the [110] oriented surface, we show the k_Y -resolved SDOS of the [110] surface in Fig. 6, where k_Y denotes the momentum parallel to the [110] surface. The k_Y -resolved SDOS is enhanced at $k_Y \sim \pm\sqrt{2}\pi/4, \pm 3\sqrt{2}\pi/4$, which correspond to $(k_x, k_y) = (0, \pm\pi/2), (\pm\pi/2, 0), (\pm\pi, \pm\pi/2), (\pm\pi/2, \pm\pi)$ at the original Fermi surface as shown in the inset of Fig. 6. At these points, angle resolved SDOS has a large value. Furthermore, quasiparticles feel a different sign of the gap

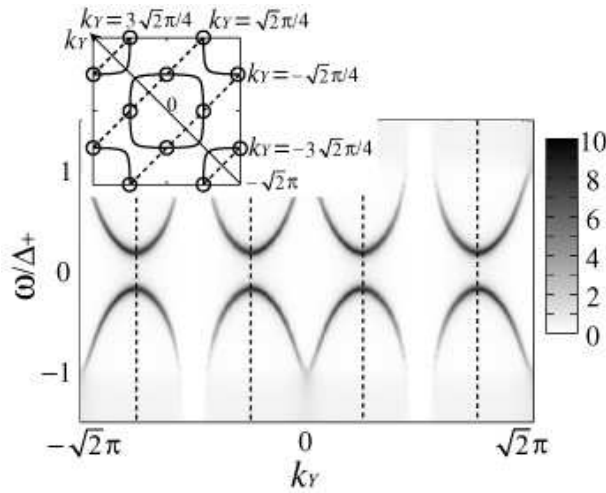


FIG. 6: Contour plot of the k_y -resolved LDOS(SDOS) in the [110] oriented surface for $n = 1$, $t' = 0.1$, and $\Delta_- = -\Delta_+ = -0.1$ (s_{\pm} -wave), where $k_y = \pm\sqrt{2}/4$ and $k_y = \pm 3\sqrt{2}/4$ are depicted as dotted lines. In the inset denote points on the Fermi surface with $k_y = \pm\sqrt{2}/4$ and $k_y = \pm 3\sqrt{2}/4$, which mainly contribute to the LDOS.

function through the scattering between inner and outer bands, which brings about the ABS. The large momentum change in quasiparticles is automatically induced by infinite potential barriers inserted at the surface due to normal (backward) reflection.

On the other hand, the k_y -resolved SDOS in the [100] surface (not shown) is enhanced at $k_y = \pm\pi/2$ within the gap. Since scattering of the quasiparticle preserving $k_y = \pm\pi/2$ occurs between the inner and outer Fermi surfaces, ABS appears within the bulk energy gap, which makes residual LDOS, shown as the dashed-dotted line in Fig. 5.

Although the sign change in the gap function does not produce the ZEP as in the case of unconventional superconductors such as d - or p -wave pairing, the sign change in the gap function felt by quasiparticle enhances the magnitude of the inner gap LDOS. In a certain case, it produces sharp peaks, shown as a solid line in Fig. 5. In order to confirm whether the above behaviors are robust or not, we change the shape of the Fermi surface by controlling the value of t' for $n = 1$, $\Delta_- = -\Delta_+ = -0.1$. As shown in Fig. 7, the positions of the two peaks in SDOS for the [110] oriented surface (solid line) move toward that of bulk LDOS (dotted line) as the value of t' increases. Thus, we find that the positions of peaks of the [110] oriented SDOS are sensitive to the shape of the Fermi surface. The resulting peak positions are relevant to the relative position between the outer and inner Fermi surface.

It is also interesting to clarify how the above results are influenced by changing the value of Δ_- . In Fig. 8, we focus on the Δ_- dependence of SDOS and bulk LDOS for $\Delta_+ = 0.1$, $n = 1$ and $t' = 0.1$. Two-gap structure

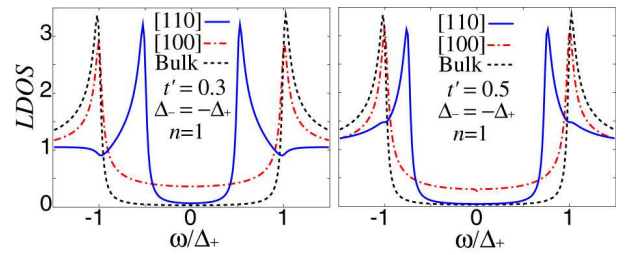


FIG. 7: (Color online) Plots of LDOS similar to Fig. 3 for $n = 1$, $\Delta_- = -\Delta_+ = -0.1$, $t' = 0.3$ (left panel) and $t' = 0.5$ (right panel).

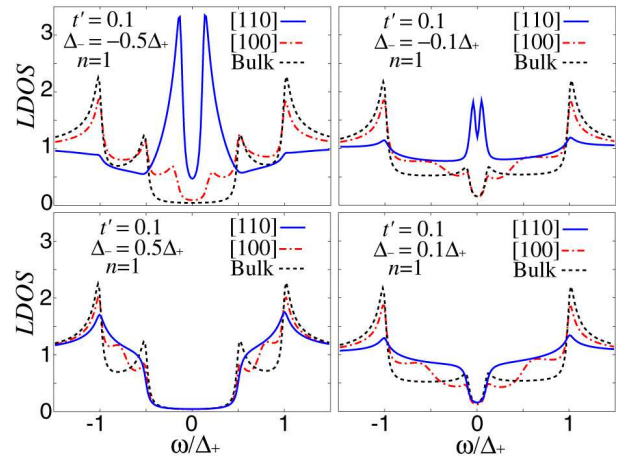


FIG. 8: (Color online) Plots of LDOS similar to Fig. 3 for $n = 1$, $t' = 0.1$, $\Delta_- = -0.5\Delta_+$ (top left panel), $\Delta_- = -0.1\Delta_+$ (top right panel), $\Delta_- = 0.5\Delta_+$ (bottom left panel), and $\Delta_- = 0.1\Delta_+$ (bottom right panel).

appears in bulk LDOS (dotted lines). It is very clear that the resulting bulk LDOS is insensitive to the sign of Δ_- by comparing the $\Delta_- = 0.5\Delta_+$ ($\Delta_- = 0.1\Delta_+$) case with the $\Delta_- = -0.5\Delta_+$ ($\Delta_- = -0.1\Delta_+$) case. As far as we are looking at bulk LDOS, there is no difference between s_{\pm} -wave and s -wave. The internal phase degree of the gap function does not appear in the bulk LDOS. On the other hand, sharp peaks of ABS appear only for SDOS of the [110] oriented surface with $\Delta_- = -0.5\Delta_+$ and $\Delta_- = -0.1\Delta_+$. The position of the sharp peaks moves toward $\omega = 0$ with the decrease of the magnitude of Δ_- . At the same time the height of the peaks is reduced (solid lines in the upper two panels). On the other hand, SDOS for the [100] oriented surface does not have clear peaks as compared to that for the [110] oriented surface.

Finally, we show the result of $n = 1.2$ for $t' = 0.1$ and $\Delta_- = -\Delta_+ = -0.1$ in Fig. 9. In this case, SDOS for the [110] oriented surface has two peaks at $\omega = \pm\Delta_+$ in addition to the two inner gap peaks. This is understood by using the k_y -resolved SDOS in Fig. 10. We see that ABS within gap vanishes for $-2\sqrt{2}\pi/3 < k_y < -\sqrt{2}\pi/3$ and $\sqrt{2}\pi/3 < k_y < 2\sqrt{2}\pi/3$ since interband pair scat-

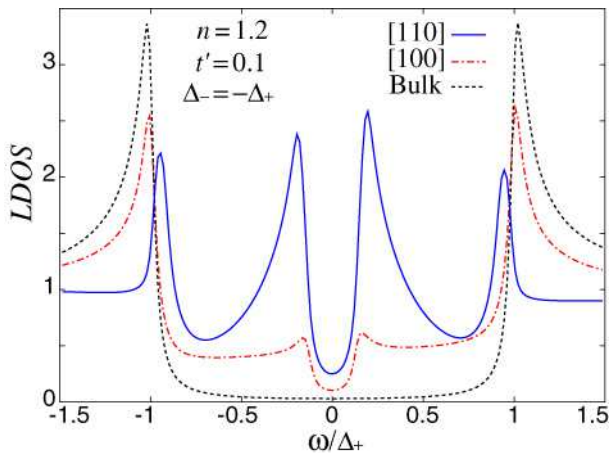


FIG. 9: (Color online) Plots of LDOS similar to Fig. 3 for $n = 1.2$, $t' = 0.1$, $\Delta_- = -\Delta_+ = -0.1$.

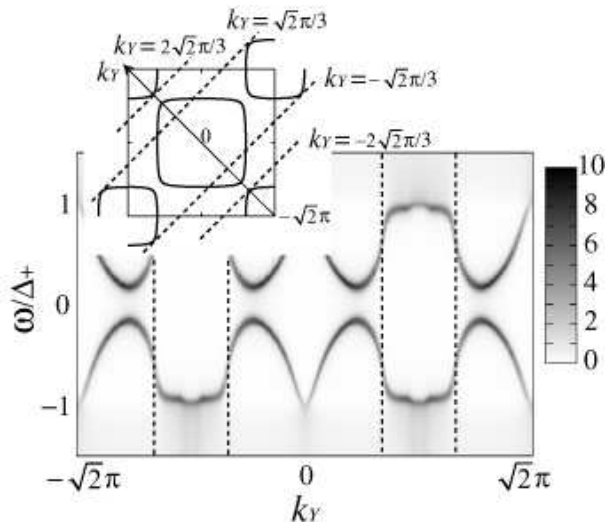


FIG. 10: Contour plot of the k_Y -resolved LDOS (SDOS) in the [110] oriented surface for $n = 1.2$, $t' = 0.1$, and $\Delta_- = -\Delta_+ = -0.1$, where $k_Y = \pm\sqrt{2}\pi/3$ and $k_Y = \pm 2\sqrt{2}\pi/3$ are depicted as dotted lines. In the inset we see that there is no interband pair scattering for $-\sqrt{2}\pi/3 < k_Y < \sqrt{2}\pi/3$ and $\sqrt{2}\pi/3 < k_Y < 2\sqrt{2}\pi/3$.

tering is prohibited due to the absence of outer Fermi surface as shown in the inset of Fig. 10. Thus, in this k_Y region, the angle-resolved LDOS is an independent summation of LDOS in the outer and inner Fermi surface. Then, the resulting angular averaged LDOS has peaks at $\omega = \pm\Delta_+$.

Summarizing the above results, although the quasiparticle feels a sign change of the gap function for fixed k_Y (k_y) in the reflection process at the surface, ZEP does not appear in the SDOS of s_{\pm} -wave pairing. Thus, ZBCP in tunneling spectroscopy appears neither the [100] nor the [110] oriented junctions. These features

are completely different from the d -wave gap function in high- T_c cuprates where ZBCP appears for the [110] orientation^{26,27,28,38}. One of the big difference from the d -wave case is that quasiparticles do not feel the sign change in the gap function as far as it is scattered within the same band in s_{\pm} -wave pairing. There are always both intraband and interband pair scattering. The presence of intraband scattering without a sign change may prohibit the generation of MABS and ZEP of SDOS. In the present study, we employ a simple two-band model. We admit that five orbitals are needed to describe the superconductivity of iron-based superconductors. Our final goal is to establish a theory of tunneling spectroscopy / surface density of state taking into account five bands. However, up to now, there has not been fully microscopic theory of surface density of states of multi-band superconducting systems even in two-bands cases. To understand the essence of the interference effects originating from the existence of the multiband, it is reasonable to start with the two-band model. Thus, in the present paper, we have chosen the two-band model for the first step as a prototype of multiband model. In the near future, we will report the results based on the more realistic five-band model.

Finally, we comment about the relevance of the present s_{\pm} -wave model in two-band systems and two-band model in non-centrosymmetric superconductors³⁹. Recently, there are several studies about surface density of states of non-centrosymmetric superconductors. The presence of the Rashba spin-orbit coupling induces Fermi surface splitting, and a similar situation in the present two-band model seems to be realized. Due to the presence of Rashba interaction, the spatial inversion symmetry is broken in these systems. Then spin-singlet s -wave and spin-triplet p -wave pairing can mix each other. If the magnitude of the p -wave component is larger than that of s -wave one, ABS exists and MABS is possible for the perpendicular injection of the quasiparticle. The resulting ABS can be regarded as helical edge modes and carry spin current. The direction of the current flow corresponding to each Kramers doublet is opposite. On the other hand, the profile of the ABS in the present two-band s_{\pm} -wave model is very different. In the present case, there is no spin current and spin degeneracy remains.

IV. CONCLUSIONS

In this paper, we have calculated the [100] and the [110] oriented SDOSs for s_{\pm} -pairing in a two-band model by changing the shape of the Fermi surface and the band filling. It has been revealed that the inner gap sharp peaks appear for SDOS in the [110] oriented surface. These peaks originate from the ABS caused by the interband scattering of quasiparticles, through which gap functions change sign. Such sharp peaks do not appear in the s -wave case, where there is no sign change in the gap function between the two bands. It is also noted that the

resulting SDOS of s_{\pm} model does not have ZEP. This means that the tunneling spectroscopy of s_{\pm} superconducting state is much more complex as compared to the d -wave case realized in high- T_c cuprates.

Up to now, there has been experimental reports about tunneling spectroscopy. The experimental line shapes of tunneling conductance are distributed including gap structures^{15,16,17,21} and ZEP^{18,19,20}. However, the experimental condition has not been clarified yet up to now. In the light of the study of high T_c cuprate^{40,41}, it has been revealed that well-oriented surface or well-oriented interface with low transparency junctions are needed to compare the surface density of states with the actual tunneling conductance⁴². We hope tunneling spectroscopy of well-oriented surface or well-controlled junctions with low transparency will be attainable in the present iron-based superconductors by the progress of microfabrication technique.

There are several interesting future problems. In the present paper, we have solved the Green's function in tight-binding model. It is possible to solve the Bogoliubov de-Gennes equation in the lattice model. The study

along this direction is useful to elucidate interference effect much more in detail^{43,44}. Josephson effect in the s_{\pm} -wave superconductor may be fascinating since we can detect internal phase effect^{45,46}. It is interesting to clarify the possible existence of nonmonotonic temperature dependence in high- T_c cuprate junctions^{47,48}. Proximity effect in s_{\pm} -wave superconductors is also an interesting topic. Through the study of the proximity effect in unconventional superconductors⁴⁹, the odd-frequency pairing amplitude has a crucial role to characterize the bound state⁵⁰. It is a challenging issue to clarify the induced odd-frequency pairing near the present two-band model.

Acknowledgments

We are grateful to A. A. Golubov and Y. Nagai for useful comments and discussions. Numerical calculations have been performed at the facilities of the Information Technology Center, University of Tokyo, and also at the Supercomputer Center, ISSP, University of Tokyo. This study has been supported by Grants-in-Aid for the 21st Century COE "Frontiers of Computational Science."

-
- ¹ Y. Kamihara, T. Watanabe, M. Hirano, H. Hosono, *J. Am. Chem. Soc.* **130**, 3296 (2008).
- ² M. Rotter, M. Tegel, D. Johrendt, *Phys. Rev. Lett.* **101**, 107006 (2008).
- ³ F. C. Hsu, J. Y. Luo, K. W. Yeh, T. K. Chen, T. W. Huang, P. M. Wu, Y. C. Lee, Y. L. Huang, Y. Y. Chu, D. C. Yan, M. K. Wu, *Proc. Nat. Acad. Sci. USA.* **105**, 14262 (2008).
- ⁴ D. J. Singh, M.-H. Du, *Phys. Rev. Lett.* **100**, 237003 (2008).
- ⁵ G. Xu, W. Ming, Y. Yao, X. Dai, Z. Fang, *Europhys. Lett.* **82**, 67002 (2008).
- ⁶ G. Mu, X. Zhu, L. Fang, L. Shan, C. Ren, H. Wen, *Chin. Phys. Lett.* **25**, 2221 (2008).
- ⁷ L. Boeri, O. V. Dolgov, A. A. Golubov, *Phys. Rev. Lett.* **101**, 026403 (2008).
- ⁸ K. Kuroki, S. Onari, R. Arita, H. Usui, Y. Tanaka, H. Kontani, H. Aoki, *Phys. Rev. Lett.* **101**, 087004 (2008).
- ⁹ I. I. Mazin, D. J. Singh, M. D. Johannes, M. H. Du, *Phys. Rev. Lett.* **101**, 057003 (2008).
- ¹⁰ D. Parker, O. V. Dolgov, M. M. Korshunov, A. A. Golubov, I. I. Mazin, *Phys. Rev. B* **78**, 134524 (2008).
- ¹¹ T. Nomura, *J. Phys. Soc. Jpn.* **77** Suppl. C, 123 (2008); arXiv:0811.2462.
- ¹² H. Ikeda, *J. Phys. Soc. Jpn.* **77**, 123707 (2008).
- ¹³ Y. Yanagi, Y. Yamakawa, and Y. Ono, *J. Phys. Soc. Jpn.* **77**, 123701 (2008).
- ¹⁴ Y. Nakai, K. Ishida, Y. Kamihara, M. Hirano, H. Hosono, *J. Phys. Soc. Jpn.* **77**, 073701 (2008).
- ¹⁵ A. Kawabata, S. C. Lee, T. Moyoshi, Y. Kobayashi, M. Sato, *J. Phys. Soc. Jpn.* **77**, 103704 (2008).
- ¹⁶ K. Hashimoto, T. Shibauchi, T. Kato, K. Ikada, R. Okazaki, H. Shishido, M. Ishikado, H. Kito, A. Iyo, H. Eisaki, S. Shamoto, Y. Matsuda, *Phys. Rev. Lett.* **102**, 017002 (2009).
- ¹⁷ L. Malone, J. D. Fletcher, A. Serafin, A. Carrington, N. D. Zhigadlo, Z. Bukowski, S. Katrych, J. Karpinski, arXiv:0806.3908.
- ¹⁸ L. Shan, Y. Wang, X. Zhu, G. Mu, L. Fang, C. Ren, H. Wen, *Europhys. Lett.* **83**, 57004 (2008).
- ¹⁹ K. A. Yates, L. F. Cohen, Z. A. Ren, J. Yang, W. Lu, X. L. Dong, Z. X. Zhao, *Super. Sci. Tech.* **21**, 092003 (2008); K. A. Yates, K. Morrison, J. A. Rodgers, G. B. S. Penny, J. W. G. Bos, J. P. Attfield, L. F. Cohen, *New J. Phys.* **11**, 025015 (2009).
- ²⁰ O. Millo, I. Asulin, O. Yuli, I. Felner, Z. A. Ren, X. L. Shen, G. C. Che, Z. X. Zhao, *Phys. Rev. B* **78**, 092505 (2008).
- ²¹ T. Y. Chen, Z. Tesanovic, R. H. Liu, X. H. Chen, C. L. Chien, *Nature* **453**, 1224 (2008).
- ²² C. C. Tsuei, J. R. Kirtley, *Rev. Mod. Phys.* **72**, 969 (2000).
- ²³ M. Sigrist, T. M. Rice, *Rev. Mod. Phys.* **67**, 503 (1995).
- ²⁴ D. J. Van Harlingen, *Rev. Mod. Phys.* **67**, 515 (1995).
- ²⁵ Y. Tanaka, S. Kashiwaya, *Phys. Rev. B* **56**, 892 (1997).
- ²⁶ C. R. Hu, *Phys. Rev. Lett.* **72**, 1526 (1994).
- ²⁷ Y. Tanaka, S. Kashiwaya, *Phys. Rev. Lett.* **74**, 3451 (1995).
- ²⁸ S. Kashiwaya, Y. Tanaka, *Rep. Prog. Phys.* **63**, 1641 (2000).
- ²⁹ Y. Tanuma, K. Kuroki, Y. Tanaka, and S. Kashiwaya, *Phys. Rev. B* **68**, 214513 (2003).
- ³⁰ Y. Bang, H. Y. Choi, and H. Won, *Phys. Rev. B* **79**, 054529 (2009).
- ³¹ P. Ghaemi, F. Wang, and A. Vishwanath, arXiv:0812.0015.
- ³² H. Y. Choi and Y. Bang, arXiv:0807.4604.
- ³³ J. Linder and A. Sudbo, *Phys. Rev. B* **79**, 020501(R) (2009).
- ³⁴ W. F. Tsai, D. X. Yao, B. A. Bernevig, and J. P. Hu, arXiv:0812.0661.

- ³⁵ X. Y. Feng and T. K. Ng, arXiv:0812.1068.
- ³⁶ A.A. Golubov, A. Brinkman, O.V. Golubov, I.I. Mazin, and Y. Tanaka, arXiv:0812.5057.
- ³⁷ Y. Nagai and N. Hayashi, arXiv:0903.1227.
- ³⁸ M. Matsumoto, H. Shiba, J. Phys. Soc. Jpn. **64**, 1703 (1995).
- ³⁹ C. Iniotakis, N. Hayashi, Y. Sawa, T. Yokoyama, U. May, Y. Tanaka, and M. Sigrist, Phys. Rev. B **76**, 012501 (2007); A. B. Vorontsov, I. Vekhter, and M. Eschrig, Phys. Rev. Lett. **101**, 127003 (2008); Y. Tanaka, T. Yokoyama, A. V. Balatsky, N. Nagaosa, Phys. Rev. B **79** 060505(R) 2009.
- ⁴⁰ L. Alff, H. Takashima, S. Kashiwaya, N. Terada, H. Ihara, Y. Tanaka, M. Koyanagi, and K. Kajimura, Phys. Rev. B **55**, R14757 (1997); J. Y. T. Wei, N. -C. Yeh, D. F. Garrigus, and M. Strasik, Phys. Rev. Lett. **81**, 2542 (1998);
- ⁴¹ I. Iguchi, W. Wang, M. Yamazaki, Y. Tanaka, and S. Kashiwaya, Phys. Rev. B **62**, R6131 (2000).
- ⁴² Y. Tanaka and S. Kashiwaya, Phys. Rev. B **53** 9371 (1996); S. Kashiwaya, Y. Tanaka, M. Koyanagi, and K. Kajimura, Phys. Rev. B **53**, 2667 (1996).
- ⁴³ Y. Tanuma, Y. Tanaka, M. Ogata and S. Kashiwaya, J. Phys. Soc. Jpn. **67**, 1118 (1998).
- ⁴⁴ Y. Tanuma, Y. Tanaka, M. Ogata and S. Kashiwaya, Phys. Rev. B **60**, 9817 (1999).
- ⁴⁵ D. Inotani and Y. Ohashi, arXiv:0901.1718.
- ⁴⁶ Y. Ota, M. Machida, T. Koyama, and H. Matsumoto, arXiv:0903.0421.
- ⁴⁷ Y. Tanaka and S. Kashiwaya, Phys. Rev. B **53**, R11957 (1996).
- ⁴⁸ Y. Tanaka and S. Kashiwaya, J. Phys. Soc. Jpn. **68**, 3485 (1999); Y. Tanaka and S. Kashiwaya, J. Phys. Soc. Jpn. **69**, 1152 (2000).
- ⁴⁹ Y. Tanaka and S. Kashiwaya, Phys. Rev. B **70**, 012507 (2004). Y. Tanaka, Y. V. Nazarov and S. Kashiwaya, Phys. Rev. Lett. **90**, 167003 (2003).
- ⁵⁰ Y. Tanaka and A. A. Golubov, Phys. Rev. Lett. **98**, 037003 (2007); Y. Tanaka, A. A. Golubov, S. Kashiwaya, and M. Ueda, Phys. Rev. Lett. **99**, 037005 (2007).